Journal of Applied Microbiology, 2024, 135, lxae173
https://doi.org/10.1093/jambio/lxae173
Advance access publication date: 11 July 2024
Research Article

JOURNAL OF APPLIED MICROBIOLOGY
OXFORD UNIVERSITY PRESS

Identification of mechanisms modulating chlorhexidine and octenidine susceptibility in *Proteus mirabilis*

Harriet Pelling[1,2,‡], Vicky Bennett[1,‡], Lucy J. Bock[3], Matthew E. Wand[3], Emma L. Denham[1], Wendy M. MacFarlane[2], J. Mark Sutton[3], Brian V. Jones[1,*]

[1]Department of Life Sciences, University of Bath, Bath BA2 7AY, United Kingdom
[2]School of Applied Sciences, University of Brighton, Brighton BN2 4GJ, United Kingdom
[3]United Kingdom Health Security Agency, Salisbury, United Kingdom

*Corresponding author. Department of Life Sciences, University of Bath, Claverton Down, BA2 7AY. E-mail: B.V.Jones@bath.ac.uk
‡These authors contributed equally.

Abstract

Aims: We aimed to identify mechanisms underlying the tolerance of *Proteus mirabilis*—a common cause of catheter associated urinary tract infection—to the clinically used biocides chlorhexidine (CHD) and octenidine (OCT).

Methods and results: We adapted three clinical isolates to grow at concentrations of 512 μg ml^{-1} CHD and 128 μg ml^{-1} OCT. Genetic characterization and complementation studies revealed mutations inactivating the *smvR* repressor and increasing *smvA* efflux expression were associated with adaptation to both biocides. Mutations in *mipA* (encoding the MltA interacting protein) were less prevalent than *smvR* mutations and only identified in CHD adapted populations. Mutations in the *rppA* response regulator were exclusive to one adapted isolate and were linked with reduced polymyxin B susceptibility and a predicted gain of function after biocide adaptation. Biocide adaptation had no impact on crystalline biofilm formation.

Conclusions: SmvR inactivation is a key mechanism in both CHD and OCT tolerance. MipA inactivation alone confers moderate protection against CHD, and *rppA* showed no direct role in either CHD or OCT susceptibility.

Impact Statement

These findings support the hypothesis that the SmvA efflux system is a key modulator of cationic biocide susceptibility in many Gram-negative pathogens and reveal additional mechanisms linked to the adaptation of *Proteus mirabilis* to cationic biocides.

Keywords: biocide tolerance; *Proteus mirabilis*; urinary tract infection; chlorhexidine; octenidine

Introduction

Antibiotic resistance is a global health concern with rising cases of treatment failure (WHO 2017). It has been estimated that globally in 2019, 4.95 million deaths were associated with drug-resistant infections (Murray et al. 2022). A key component of tackling antibiotic resistance is enhanced infection prevention, where biocides are an essential component (Gilbert and Moore 2005, Maillard 2005). These important antimicrobial agents are used as antiseptics and disinfectants and often employed to remove microbes from surfaces, equipment, and patients' skin to prevent infection. The rising incidence of antibiotic resistance, and more recently the SARS-CoV-2 pandemic, has increased the use of biocides in clinical settings as part of enhanced infection control measures (Wand et al. 2016, Wand et al. 2019, Rawson et al. 2020, Zheng et al. 2020). However, biocides are poorly regulated in the UK compared to therapeutic agents such as antibiotics, and they are used without clear evidence or indication in many cases (Harbarth et al. 2014, Kampf 2016, Lai et al. 2016, Slipski et al. 2018). Commensurately, this has given rise to concerns that the inappropriate use of these important compounds may undermine their clinical value and potentially select for reduced susceptibility and antibiotic cross-resistance in problematic pathogens.

The cationic biocide chlorhexidine (CHD) is currently one of the most widely used biocides in the UK and is indicated in the prevention of surgical site infections and healthcare-associated infections in general (NICE 2017, 2020, Coia et al. 2021). Furthermore, CHD has been declared an essential medicine as an antiseptic by the World Health Organization (WHO 2021). Octenidine (OCT) is becoming an increasingly popular alternative to CHD having been shown to be less cytotoxic with a similar mode of action and spectrum of activity (Schmidt et al. 2016, 2018, Coaguila-Llerena et al. 2020). Both biocides are found in a wide range of products, including body cleansers, oral hygiene products, wound treatments, and urinary catheter irrigation solutions at concentrations from 0.02% to 4% for CHD and 0.025%–1% for OCT (Russell 1986, McDonnell and Russell 1999, Gilbert and Moore 2005, Lim and Kam 2008, Atiyeh et al. 2009, Lambert 2012, Kampf 2016, Hardy et al. 2018, Slipski et al. 2018, Schülke and Mayr UK Ltd 2021). It has been speculated that these varied concentrations and wide range of uses lead to sublethal concentrations of CHD or OCT in healthcare settings that could select for reduced susceptibility and other undesirable traits among bacterial pathogens (Bock et al. 2016).

Proteus mirabilis is an opportunistic pathogen that poses particular problems in catheter associated urinary tract

Received 10 May 2024; **revised** 20 June 2024; **accepted** 10 July 2024

infections (CAUTI) due to its ability to form crystalline biofilms (Stickler et al. 1993, Morris and Stickler 1998, Jacobsen et al. 2008, Stickler and Feneley 2010). *Proteus mirabilis* is also often described as 'innately resistant' to CHD, with the isolation of strains able to tolerate relatively high concentrations of CHD documented since the late 1960s (Gillespie et al. 1967, O'Flynn and Stickler 1972, Stickler,1974, Stickler and Thomas 1980, Southampton Infection Control Team 1982, Walker and Lowes 1985, Dance et al. 1987, Stickler et al. 2002). However, previous studies have demonstrated that CHD minimum inhibitory concentrations (MIC) can vary considerably between *P. mirabilis* isolates (up to 64-fold), indicating high tolerance to this biocide is acquired by *P. mirabilis* (Pelling et al. 2019). Nevertheless, the mechanisms underpinning acquisition of reduced susceptibility to CHD remain poorly defined, and it is unclear if susceptibility to other antimicrobial agents is also modulated by these mechanisms. Here, we employ an adaptive evolution approach to further elucidate the mechanisms leading to reduced CHD and OCT susceptibility in *P. mirabilis*. In doing so, we identify key mutations and common mechanisms that underpin adaptation of *P. mirabilis* to tolerate increasing concentrations of these cationic biocides.

Materials and methods

General culture and media

The *P. mirabilis* clinical isolates used in this study were obtained from the Royal Sussex County Hospital and Bristol Southmead Hospital. Bacteria were cultured in Lysogeny broth (LB) (10 g l^{-1} tryptone, 5 g l^{-1} yeast extract, and 10 g l^{-1} sodium chloride) or tryptic soya broth (TSB) (17 g l^{-1} pancreatic digest of casein, 3 g l^{-1} enzymatic digest of soya bean, 5 g l^{-1} sodium chloride, 2.5 g l^{-1} dipotassium hydrogen phosphate, and 2.5 g l^{-1} glucose) at 37°C with aeration. For growth on solid media for isolation of single colonies, LB agar without salt (1.5% wt vol^{-1} agar) or MacConkey number 3 agar was used.

Determination of MIC

The MIC of CHD (Sigma-Aldrich) and OCT (Schülke & Mayr) was determined using a broth microdilution method in 96-well polypropylene plates (Greiner Bio-One) for cationic compounds (Bock et al. 2018), and antibiotic MIC values were obtained in accordance with European Committee on Antimicrobial Susceptibility Testing (EUCAST) guidelines in 96-well polystyrene plates (Corning).

Adaptation of *P. mirabilis* to biocides

Proteus mirabilis isolates B4, RS1, and RS50a were adapted to grow at increasing concentrations of chlorhexidine digluconate (CHD, 8–512 μg ml^{-1}) (chlorhexidine digluconate solution, Sigma-Aldrich), or octenidine dihydrochloride (OCT, 2–128 μg ml^{-1}, Schülke & Mayr) as described previously (Bock et al. 2016). Aliquots of 50 μl overnight culture were used to inoculate 3 ml of TSB supplemented with the starting concentration of biocide and incubated at 37°C. After 48 h of incubation, 50 μl of the initial culture was transferred to 3 ml of fresh TSB with double the previous concentration of biocide and incubation continued. This process was repeated for 14 days alongside a non-biocide exposed control (NBC). Cells surviving the highest concentrations tested were passaged 10 times on tryptic soya agar in the absence of biocide. Following the 10th passage, the MIC was tested again to confirm a stable tolerant phenotype, and the biocide adapted population, NBC population, and 10 single colonies from each biocide adapted population were stored in Microbank™ vials (Pro-Lab Diagnostics) at −80°C.

Genome sequencing and identification of biocide-associated mutations

Biocide adapted isolates were genetically characterized to identify mutations selected for by biocide adaptation. DNA was extracted from selected sub-isolates of interest using a Wizard Genomic DNA Purification Kit (Promega) as per the manufacturer's instructions, with DNA rehydration being carried out overnight at 4°C in the provided rehydration solution. Genomic DNA was diluted to ∼20 ng μl^{-1} as measured using a Qubit flurometer (Invitrogen) and used for generation of whole genome sequences using the UKHSA-GSDU (United Kingdom Health Security Agency Genomic Services and Development Unit) lllumina HiSeq 2500 and Galaxy online platform as previously described (Wand et al. 2016, 2019, Afgan et al. 2018). A minimum of 150 Mb of Q30 quality data was obtained for each sample and reads subject to trimming as previously described (Wand et al. 2016, Prjibelski et al. 2020). To identify biocide associated mutations, trimmed reads from adapted sub-isolates and their respective parental strains were mapped to the *P. mirabilis* HI4320 (NC_010 554) reference genome using BBMap (v38.84) (https://sourceforge.net/projects/bbmap) and polymorphisms were predicted using Freebayes (v1.1.0) with variant detection settings set to a minimum coverage of 10 and minimum variant frequency of 0.1 (Garrison and Marth 2012). InterProScan (Blum et al. 2021), implemented in Geneious Prime 2019.2.1 (https://www.geneious.com), was used to predict putative protein domains. Parental genome sequences are available in GenBank (BioProject accession number PRJNA554808).

Complementation

A CHD adapted RS50a isolate and an OCT adapted RS50a isolate were selected for complementation with wild type (WT) *smvR*.Plasmids were extracted from RS47::pGEM-Tempty and RS47::RS50A*smvR*, generated in Pelling et al. (2019), using a QIAprep Spin Miniprep Kit (Qiagen) and were subsequently introduced to *P. mirabilis* isolates by electroporation (0.1-cm gap cuvettes, 1.25 V, 25 μF, 200 Ω). Cells were recovered in super optimal broth medium (20 mmol l^{-1} glucose, 10 mmol l^{-1} MgCl2, 10 $mmol^{-1}$ MgSO4, 2.5 $mmol^{-1}$ KCl, 10 $mmol^{-1}$ NaCl, 20 g l^{-1} tryptone, and 5 g l^{-1} yeast extract) for 1 h at 37°C with shaking, before selection of transformed colonies on non-swarming LB agar supplemented with 100 μg ml^{-1} ampicillin.

Measurement of *smvA* expression

Expression of *smvA* was measured by quantitative PCR as previously described using primers smvAF and smvAR (Table 5; Pelling et al. 2019). Briefly, 9 ml LB was inoculated with 1 ml of overnight culture, which was grown for 3 h to mid-log phase. The culture was pelleted, washed in PBS, and resuspended in a final volume of 200 μl PBS. RNA was extracted from this final cell suspension using the RNeasy PowerMicrobiome Kit (Qiagen) according to manufacturer's

instructions, including the optional phenol-chloroform-isoamyl alcohol step. RNA extracts were treated using the DNase MAX Kit (Qiagen) according to manufacturer's instructions to remove contaminating genomic DNA before cDNA generation using the QuantiTect RT Kit (Qiagen). qPCR was carried out using a Rotor-Gene Q cycler with the Rotor-Gene SYBR® Green PCR Kit (Qiagen) according to the manufacturer's instructions. Each 25 μl reaction contained 12.5 μl 2x Rotor-Gene SYBR Green PCR master mix containing HotStarTaq Plus DNA Polymerase, Rotor-Gene SYBR Green PCR Buffer, and SYBR Green I dye; 1 μl primer mix (10 pmol per primer); 100 ng cDNA template. Reactions were brought to a final volume of 25 μl with nuclease free water. Duplicate technical replicates were run for each biological replicate, and negative controls consisted of reactions containing no template cDNA and DNase treated RNA. A calibration curve of DNA standards (pGEM-T easy vector harbouring a fragment of *smvA* from *P. mirabilis* B4) was included in each replicate experiment to permit quantification of *smvA* transcripts.

Analysis of mutations in biocide adapted populations using the breseq pipeline

As previously described (Pelling et al. 2019), total genomic DNA from each adapted culture was extracted using the Wizard Genomic DNA Purification Kit (Promega). To amplify *smvR*, *mipA*, and *rppA*, hi-fidelity DreamTaq Green PCR Master Mix (Thermo Scientific) was used with corresponding primers (Table 5) (10 pmol/primer) in 50 μl reactions with ~10–20 ng DNA template. The resulting amplicons were purified using a QIAquick PCR Purification Kit (Qiagen) and sequenced by UKHSA-GSDU on an Illumina HiSeq 2500 instrument, with a minimum of 150 Mb of Q30 quality data obtained for each culture. Raw reads were adaptor and quality trimmed using fastP (v0.23.4) (Chen et al. 2018) to obtain sequences of a minimum length of 20 bp and a minimum quality of 10. Sequences corresponding to regions flanking the genes of interest were filtered out using SAMtools (v1.13) (Danecek et al. 2021). To identify mutations, the trimmed and filtered amplicon sequences from the adapted populations were compared with the parental reference sequence using the breseq (v0.38.1) pipeline (Bowtie2 v2.5.1; R v4.3.1) in polymorphism mode with no filters and with targeted mapping applied (Deatherage and Barrick 2014).

In vitro models of the catheterized urinary tract

Bladder models representative of the catheterized urinary tract originally described by Stickler et al. (1999) were performed with minor modifications as described by Clarke et al. (2023) and allowed to run until catheter blockage occurred. Artificial urine (AU) was prepared as (i) an autoclaved 5 × stock solution (11.5 g l^{-1} anhydrous sodium sulfate, 3.25 g l^{-1} magnesium chloride hexahydrate, 23 g l^{-1} sodium chloride, 3.25 g l^{-1} tri-sodium citrate, 0.1 g l^{-1} sodium oxalate, 14 g l^{-1} potassium di-hydrogen orthophosphate, 8 g l^{-1} potassium chloride, 5 g l^{-1} ammonium chloride, 25 g l^{-1} gelatine, 5 g l^{-1} tryptone soy broth) and (ii) a separate filter sterilized calcium/urea solution (0.44 μM filter; 156.25 g l^{-1} urea, 3.0625 g l^{-1} calcium chloride). Solution (i) was pH adjusted to 5.75 using a pH meter (HI 2210; Hanna Instruments), then 1 l volume of (i) was combined with 400 ml of the solution (ii) and topped up to 5 l with sterile deionized water, resulting in a final pH of 6.10.

Double-walled glass vessels representing the bladder were maintained at 37°C using a circulating water bath. Silicone catheters (BARDIA® AQUAFIL® All Silicone Foley Catheter; Bard) were inserted into the inner chamber, and the balloons were inflated using 10 ml sterile water. A sterile drainage bag (BARDIA® Drainable Bed Bag with 180° lever tap; Bard) was attached to the catheter to create a closed drainage system. Models were inoculated with 10 ml of OD600 nm 1.0 (± 0.1) normalized overnight culture resuspended in 10 ml of AU (ca. 10^8 CFU ml^{-1}), and infection was allowed to establish for 1 h before starting AU flow at a constant pump rate of 3 rpm. Samples from the central chamber were taken for CFU ml^{-1} calculations and pH analysis at time of inoculation and time of blockage.

Table 1. Biocide MICs of *P. mirabilis* clinical isolates prior to adaptation.

Isolate	CHD MIC μg ml^{-1}	OCT MIC μg ml^{-1}
B4	32–64	≤8
RS1	16	≤8
RS50a	8–16	≤8

Results

Adaptation to CHD and OCT

To identify mutations and mechanisms underpinning reduced susceptibility to CHD and OCT in *P. mirabilis*, three clinical isolates (B4, RS1, and RS50a) were adapted to grow at increasing concentrations of these biocides (from 8 to 512 μg ml^{-1} for CHD; from 2 to 128 μg ml^{-1} for OCT). In comparison to other *P. mirabilis* isolates we have characterized, B4, RS1 (Pelling et al. 2019), and RS50a show high susceptibility to both biocides (Table 1). All isolates were successfully adapted to grow at the highest concentrations of CHD and OCT used (512 μg ml^{-1} CHD; 128 μg ml^{-1} OCT) and maintained an increased MIC after 10 passages on agar in the absence of biocides. In contrast, the MICs for no biocide control populations of each isolate (passaged in the absence of biocides) remained comparable with initial wild type MICs, confirming that changes in biocide susceptibility were the result of biocide exposure.

To determine if elevated biocide susceptibility varied within adapted populations, 10 single colonies derived from each WT parental isolate (B4, RS1, and RS50a) were randomly selected. These 'sub-isolates' were designated according to parental lineage and biocide to which they had been adapted, and MICs to both CHD and OCT were assessed (Supplementary Data S1). All CHD adapted sub-isolates exhibited CHD MICs of ≥512 μg ml^{-1} (Supplementary Data S1). In contrast, MICs of sub-isolates selected from OCT adapted populations ranged from 64 to 128 μg ml^{-1} in RS1 derived sub-isolates, 128–256 μg ml^{-1} in B4 derived sub-isolates, and 128–512 μg ml^{-1} in RS50a derived sub-isolates (Supplementary Data S1).

Identification and characterization of mutations associated with biocide adaptation

To identify mutations associated with biocide exposure, whole genome sequences were obtained from five sub-isolates of each lineage adapted to CHD and OCT, as

Table 2. Genetic changes in *P. mirabilis* isolates after adaptation to CHD and OCT.

Gene	Predicted function[a]	Parental isolate	Biocide adaptation[b]	Frequency of sequenced sub-isolates with mutation in gene	Mutations[c]
smvR	TetR-family transcriptional regulator (PMI_RS14640)	B4	CHD	5/5	SNP in promoter (−22)2 or (−29)2
		RS1	OCT	5/5	R5S1; T29A1
		RS50a		5/5	SNP in promoter (−10)2 or (−29)1
		B4		5/5	S98P1; L105V1
		RS1		5/5	G24R5
		RS50a		5/5	W166*2; S171*1; T91P1; 37FS > 54*1
					R69*4; A34P1 37FS > 54*5
mipA	MltA-interacting protein (PMI_RS07300)	B4	CHD	2/5	W123*1; W73*1
		RS1		2/5	239FS > 241*1
		RS50a		5/5	37FS > 40*1 31FS > 40*5
rppA	Response regulator transcription factor (PMI_RS08300)	RS50a	CHD	5/5	D211N5
			OCT	5/5	D211N5
Hypothetical regulator	helix-turn-helix transcriptional regulator (PMI_RS08455)	RS50a	OCT	1/5	K3R1
mscM	Mini-conductance mechanosensitive channel (PMI_RS16680)	RS1	OCT	1/5	A980T1
relA	GTP pyrophosphokinase (PMI_RS01045)	B4	CHD	1/5	K630*1
sdaA	L-serine ammonia-lyase (PMI_RS07845)	B4	CHD	1/5	D197A1

[a] *Proteus mirabilis* HI4320 gene identification is shown in parentheses (accession number NC_010 554). Mutations in *smvR* were most prevalent in all CHD and OCT adapted populations.
[b] CHD—chlorhexidine; OCT—octenidine.
[c] For single nucleotide polymorphisms (SNPs) in promotor regions (*-xx*) denotes position upstream from start codon. *x*FS > *x** indicates an indel leading to a frameshift at codon number *x* and premature stop codon (*) at codon number *x*. Predicted amino acid substitutions are indicated using single letter codes and codon numbers e.g. D211N indicates a change from aspartic acid to Asparagine at codon 211. Superscript numerals indicate the number of sequenced sub-isolates harbouring a particular mutation e.g. G24R5 indicates that all five sequenced sub-isolates harboured this mutation. Details of mutations in each sequenced sub-isolate can be found in Supplementary Data Set S1.

well as for associated no biocide control populations. Sub-isolates were selected at random from CHD adapted populations, while those with highest MICs were selected from OCT adapted populations (Supplementary Data S1). To identify mutations acquired following biocide adaptation reads from individual sub-isolate sequences were mapped to the respective parental WT genome sequence. Only non-synonymous mutations found in protein coding sequences or predicted promoter regions were considered in this analysis. To ensure only biocide-associated mutations were identified, comparable mutations that were also identified in sequences derived from the no biocide control population were disregarded.

Using these criteria, a total of seven genes were found to contain biocide-associated mutations in various adapted sub-isolates (Table 2; Supplementary Data S1). Genes considered to be most clearly associated with biocide adaptation were those with mutations identified in all sequenced sub-isolates of a particular lineage and/or present in multiple sub-isolates derived from all parental lineages. Based on these criteria, mutations in *smvR*, *mipA*, and *rppA* were most clearly associated with biocide adaptation, and analogous mutations in *smvR* and *mipA* were also identified in the previously characterized CHD tolerant isolated RS47 (CHD MIC ≥ 512 μg ml^{-1}; Pelling et al. 2019). Mutations in other genes identified (*sdaA*, *mscM*, *relA*, and a putative HTH regulator) were less clearly associated with biocide adaptation, and mutations in these genes were not identified in the CHD tolerant isolate RS47 (Table 2).

SmvR

Mutations in *smvR* or its promoter were the most common and observed in every biocide adapted sub-isolate sequenced, regardless of the biocide used (Table 2). This Tet-like repressor regulates expression of the cognate *smvA* efflux system, and mutations in *smvR* are already linked with CHD tolerance in RS47 (Pelling et al. 2019). Alignments of SmvR amino acid translations showed that many of these mutations are predicted to result in a truncated protein lacking some or all of the C-terminal domain, as previously observed in RS47 (Fig. 1). A range of single nucleotide polymorphisms (SNPs) were also observed in both the TetR-like DNA-binding domain and the TetR transcriptional regulator CgmR-like domain (Fig. 1). Mutations in the *smvAR* promoter were found exclusively in CHD adapted sub-isolates of B4 and RS1 lineages.

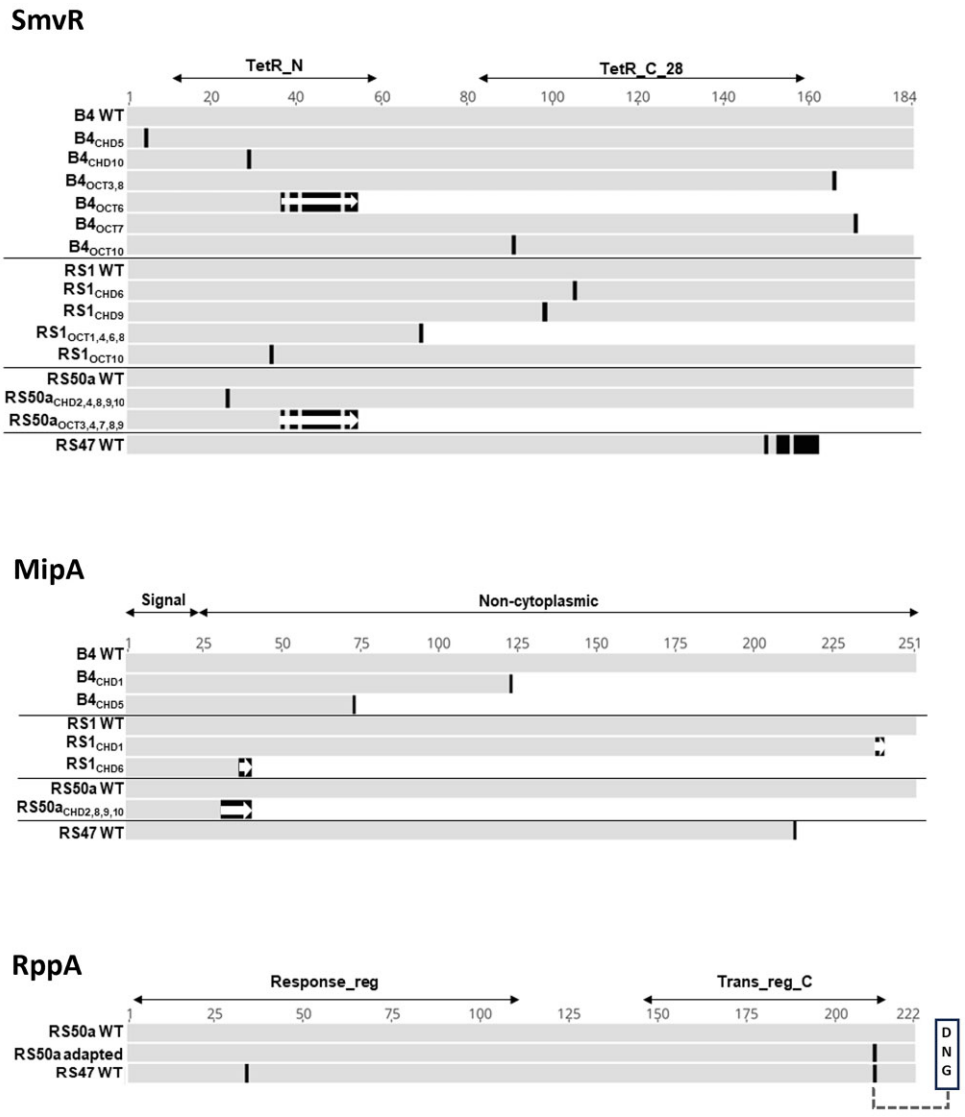

Figure 1. *Impact of biocide associated mutations on smvR, mipA, and rppA translated amino acid sequences.* Translated amino acid sequences of *smvR*, *mipA*, and *rppA* from parental WT strains, sequenced biocide adapted sub-isolates, and the previously characterized CHD tolerant RS47 WT were compared by alignments with ClustalW. Putative protein domains were determined by InterProScan. Sequences from adapted sub-isolates from each lineage (B4, RS1, and RS50a) were compared to the respective parental WT sequences. RS47 sequences were compared to the consensus sequence from WT parental isolates. *Black bars* = single amino acid changes; *White arrows* = frame shifts. For RppA alignments specific amino acids at position 211 are shown in associated annotation: D—Aspartic Acid; N—Asparagine; G—Glycine.

MipA

Mutations in *mipA* were identified in sequenced sub-isolates derived from all lineages but were only observed in sub-isolates adapted to CHD (Table 2). MipA encodes a putative scaffolding protein that interacts with murein hydrolases and polymerases during peptidoglycan synthesis or turn over, and alignments of translated amino acid sequences showed that mutations were all associated with the introduction of premature stop codons and the likely inactivation of MipA (Fig. 1). This analysis also showed the highly CHD tolerant isolate RS47 harbours a similar mutation in *mipA* predicted to lead to a stop codon at position 213 and production of a truncated protein (Fig. 1).

RppA

Mutations in the *rppA* response regulator, part of the *rppAB* two component signal transduction system, were identified only in RS50a sub-isolates but were observed in all sequenced sub-isolates from both OCT and CHD adapted populations of this lineage (Table 3). Notably, alignments of translated RppA amino acid sequences from CHD and OCT adapted RS50a sub-isolates showed all possess conserved mutations that result in an aspartic acid to asparagine substitution at position 211, predicted to be within the C-terminal DNA binding domain of this response regulator (Fig. 1). In contrast, RS1, B4, and the previously characterized RS47 were all found to encode a glycine residue at this site (Fig. 1). Additional BlastP

Table 3. Mutations in genes of interest in adapted populations are identified using breseq.

Gene	Population[a]	Mutation[b]	NT position	Protein effect[c]	Frequencies
smvR	$B4_{CHD}$	G > T	−10	SNP in	29.3%
		A > G	−29	promoter	34.4%
		A > G	92	SNP in	6.1%
		T > G	530	promoter	7.7%
				T29A	
				L177R	
	$B4_{OCT}$	A(7)>A(6)	109	37FS > 54*	10.1%
		A > C	310	S104R	6.7%
		A > C	271	T91P	10.2%
		G > A	497	W166*	22.5%
		T(6)>T(5)	434	L145*	18.9%
		T(5)>T(6)	511	S171*	14.9%
	$RS1_{CHD}$	G > T	−10	SNP in	24%
		A > G	−29	promoter	19.3%
		C > T	10	SNP in	6.3%
		T > C	292	promoter	20.2%
		T > G	313	Q4*	19.7%
				S98P	
				L105V	
	$RS1_{OCT}$	G > T	4	G2*	6.7%
		C > T	205	R69*	87.1%
	$RS50a_{CHD}$	G > A	70	G24R	100%
	$RS50a_{OCT}$	(A)7>(A)6	103	37FS > 54*	85.2%
mipA	$B4_{CHD}$	A > C	730	T244P	24.2%
		G > A	369	W123*	26.6%
	$RS1_{CHD}$	G > A	368	W123*	6.6%
		$(GGGAC)_{1>2}$	658	221FS > 236*	14.4%
		+T	107	37FS > 40*	71.3%
	$RS50a_{CHD}$	(G)5>(G)6	85	31FS > 40*	100.0%
rppA	$RS50a_{CHD}$	G > A	631	D211N	100.0%
	$RS50a_{OCT}$	G > A	631	D211N	100.0%

[a]Parental lineage and biocide adaptation e.g. $B4_{CHD}$ indicated populations derived from WT B4 adapted to CHD. CHD—chlorhexidine; OCT—octenidine.
[b]*x* > *x* indicates single base substitutions (e.g. A > T). Δxxbp indicates number of bases deleted as associated nucleotide position. + indication insertion of bases at associated nucleotide position.
[c]For SNPs in promotor regions (-*xx*) denotes position upstream from start codon. *x*FS > *x** indicates an indel leading to a frameshift at codon number *x* and premature stop codon (*) at codon number *x*. Predicted amino acid substitutions are indicated using single letter codes and codon number e.g. D211N indicates a change from Aspartic acid to Asparagine at codon 211.

searches of the nr database showed that glycine at position 211 of the *P. mirabilis rppA*, and homologous proteins, is highly conserved and present in 99.4% of sequences in the top 1000 hits.

Population level analysis of biocide associated mutations

To examine the prevalence of biocide-associated mutations within the wider adapted populations of each isolate (RS1, B4, and RS50a), we undertook breseq analysis of *smvR*, *mipA*, and *rppA*. For *smvR*, in addition to the mutations identified in individual sequenced sub-isolates, biocide adapted populations from B4 and RS1 were predicted to encode further novel mutations in the promoter and in *smvR* coding regions, with predicted frequencies for individual mutations ranging between 6.1% and 87.1% (Table 4). Additional mutations leading to SNPs, insertions, and deletions in *mipA* were also identified within CHD adapted populations from B4 and RS1, with the frequencies of mutations varying between 6.6% and 71.3% in these populations (Table 4). Mutations in *smvR*, *mipA*, and *rppA* were also prevalent in RS50 populations but specific mutations appeared to be highly conserved, with a single SNP in each of these genes dominating within adapted populations (Table 3). This prediction resulted from the very low prevalence of the original parental sequence within RS50a biocide adapted populations and no detection of alternative minor variants, which resulted in Breseq designating these as clonal populations. Breseq analysis also confirmed no detectable *mipA* mutations in OCT adapted populations from any lineage, and no detectable mutations in *rppA* within adapted populations of B4 and RS1.

Impact of biocide associated mutations on antimicrobial susceptibility profiles

To determine the relative contribution of biocide associated mutations in *smvR*, *mipA*, and *rppA* to CHD and OCT susceptibility, we complemented $RS50a_{CHD8}$ and $RS50a_{OCT3}$ sub-isolates with a functional copy of *smvR* to provide RS50a derivatives with varying combinations of *rppA* and *mipA* mutations and *smvA* activity (Table 4). These strains were also used to evaluate the contribution of biocide associated mutations to antibiotic susceptibility. Quantification of *smvA* expression by RT-qPCR confirmed this was reduced to WT levels in strains complemented with functional *smvR*. Conversely, adapted sub-isolates harbouring empty vector alone ($RS50a_{CHD8::\ empty}$ and $RS50a_{OCT3::\ empty}$) exhibited at least 20-fold greater *smvA* expression ($P \geq .01$) than the RS50a WT.

In all cases, the MICs of the parental WT and NBC were comparable. For the majority of antibiotics tested, no significant differences in MICs were observed in biocide adapted

Table 4. Contribution of mutations in *smvR*, *mipA*, and *rppA* to antimicrobial susceptibility.

Strain [a]		RS50a WT::empty	RS50a NBC::empty	CHD adapted RS50a$_{CHD8}$::empty	RS50a$_{CHD8}$::*smvR*	OCT adapted RS50a$_{OCT3}$::empty	RS50a$_{OCT3}$::*smvR*
Gene status/function[b]	SmvR	ON	ON	OFF	ON	OFF	ON
	SmvA[c]	OFF	OFF	ON	OFF	ON	OFF
	MipA	ON	ON	OFF	OFF	ON	ON
	RppA	ASP	ASP	ASN	ASN	ASN	ASN
Antibiotic[d]	CHL	16–32 (R)	32–64 (R)	8–16 (R)	32–64 (R)	16 (R)	8–32 (R)
	CIP	≤0.03 (S)	≤0.03 (S)	0.06–0.125 (S)	0.06 (S)	0.06–0.125 (S)	0.06 (S)
	CST	256–512 (R)	256 (R)	>512 (R)	>512 (R)	>512 (R)	>512 (R)
	GEN	4–16 (R)	4–16 (R)	4 (R)	4–8 (R)	4–8 (R)	8–16 (R)
	LEX	32–64 (R)	32–64 (R)	32 (R)	32–64 (R)	32 (R)	64 (R)
	NAL	8–16 (NA)	8–16 (NA)	4–16 (NA)	4–16 (NA)	4–8 (NA)	4–8 (NA)
	PMB	64–256 (R)	128–256 (R)	**>16 384** (R)	**>16 384** (R)	**>16 384** (R)	**>16 384** (R)
	TMP	2–4 (S)	2 (S)	2–4 (S)	2–4 (S)	2–4 (S)	2–4 (S)
Biocide[d]	CHD	8–16	8–16	**512**	**64**	**512**	16
	OCT	2	2–4	**128**	1–4	**128–256**	2–4

[a]The RS50a WT and derivative strains were used to evaluate the relative contributions of mutations in *smvR*, *mipA*, and *rppA* to antimicrobial susceptibility as determined by minimum inhibitory concentration. **RS50a$_{CHD8}$** harbours mutations in *smvR*, *mipA*, and *rppA*. **RS50a$_{OCT3}$** harbours mutations in *smvR* and *rppA*. Control strains harboring empty pGEM-T vectors are indicated as '**:: empty**'. Strains complemented with a functional *smvR* repressor are indicated as '**:: smvR**'. (R) and (S) denote the isolate as either resistant or sensitive according to the EUCAST clinical breakpoints for each antibiotic tested. (NA) indicates there is no available breakpoint.

[b]Summary of the status of genes/products investigated in RS50a and derivatives. For ease of interpretation, the status of SmvR, SmvA, and MipA is summarized as either **ON** (active/overexpressed) or **OFF** (inactive/repressed). For the RppA response regulator, the predicted amino acid at position 211 is provided.

[c]*smvA* efflux pump expression was confirmed by RT-qPCR. No significant differences in *smvA* expression were detected between the RS50a WT, NBC, and complemented sub-isolates harboring functional *smvR* (RS50a$_{CHD8}$:: smvR, RS50a$_{OCT3}$:: smvR). Conversely, *smvA* expression in un-complemented biocide adapted sub-isolates (RS50a$_{CHD,}$ RS50a$_{CHD8}$:: empty, RS50a$_{OCT3,}$ RS50a$_{OCT3}$:: empty), was shown to be at least 20-fold greater than the RS50a WT ($P \geq .01$).

[d]CHL, chloramphenicol; CIP, ciprofloxacin; CST, colistin; GEN, gentamicin; LEX, cefalexin; NAL, nalidixic acid; PMB, polymyxin B; TMP, trimethoprim; CHD, chlorhexidine; OCT, octenidine. Significant changes (>2-fold change compared to RS50aWT:: empty) are in bold. As shown above, *SmvA* overexpression was a key factor in reduced susceptibility to both CHD and OCT. MipA inactivation was associated with moderate protection against CHD only.

Table 5. List of primers used in this study.

Primer	5′-3′ Sequence	Product
SMVA-F	TCGCCACCCTTATTGCCATT	qPCR primers for measurement of smvA expression
SMVA-R	CGGCGACTAACTGTAAGCGT	
SMVR-FLANK2-F	CGTTGCAGGCATGCTCATAG	Amplification of *smvR* for BreSeq analysis in isolates B4, RS1, and RS50a
SMVR-FLANK2-R	CGCCTCTGTGTATTCCGACT	
RPPA-FLANK-F	GTAAGAAAAGATCGCCTCTTATCTC	Amplification of *rppA* for BreSeq analysis in isolates B4, RS1, and RS50a
RPPA-FLANK-R	TTTCAGAGGCAAGCGACAGT	
MIPA-FLANK-R	TGGCATGTGTTGAAACAGCT	Amplification of *mipA* for BreSeq analysis in isolates B4, RS1, and RS50a
MIPA-FLANK-F	CTGGTGATGGTGGAATTGCA	

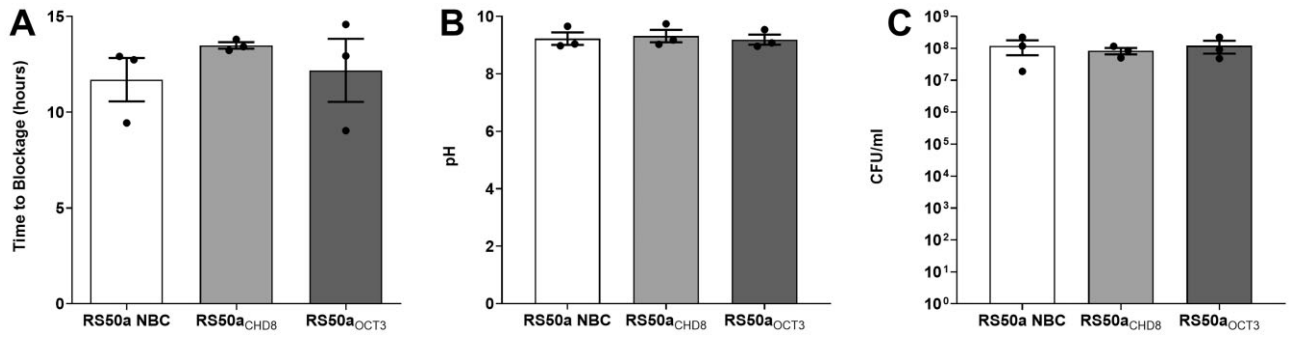

Figure 2. *Impact of biocide modulated mutations on P. mirabilis crystalline biofilm formation: In vitro* infection models simulating catheter-associated urinary tract infections demonstrated that the biocide associated mutations in RS50a$_{CHD8}$ and RS50a$_{OCT3}$ do not affect crystalline biofilm formation. (A) Time taken for catheters to block. (B) pH of residual AU at time of blockage. (C) Viable cells in residual AU at time of blockage. Data represent the mean from three replicate experiments, and error bars show standard error of the mean. No statistically significant differences in time to blockage, pH, or CFU/ml at blockage were identified.

sub-isolates, regardless of mutations harboured or *smvR* complementation (Table 4). However, both biocide adapted sub-isolates showed a ∼64-fold increase in polymyxin B (PMB) MIC. This increased PMB MIC was not associated with *smvR* expression or *mipA* mutations, indicating mutations in the *rppA* response regulator specifically are linked to this phenotype (Table 4). In contrast, the CHD and OCT MICs for the RS50a derivates tested showed that *smvR* mutations (leading to enhanced *smvA* efflux expression) are a key factor in modulation of both OCT and CHD susceptibility in RS50a (Table 5). Restoration of *smvR* activity in RS50a$_{OCT3}$ was sufficient to fully restore both CHD and OCT susceptibility, regardless of mutations in *rppA* (Table 4). However, in RS50a$_{CHD8}$, which also harbours mutations in *mipA*, complementation with *smvR* did not fully restore CHD susceptibility, indicating *mipA* mutations also contribute to modulating CHD susceptibility (Table 4).

Impact of biocide-associated mutations on crystalline biofilm formation

The blockage of urethral catheters through formation of crystalline biofilms is a key clinical complication arising from *P. mirabilis* infection. To test if biocide associated mutations affected the formation of crystalline biofilms, the ability of RS50a NBC, RS50a$_{CHD8}$ (*rppA*, *mipA*, and *smvR* mutations), and RS50a$_{OCT3}$ (*rppA* and *smvR* mutations) to block urinary catheters was compared using an *in vitro* infection model. No significant differences in time to blockage of the urinary catheters, pH of residual bladder model urine, or viable cell counts at time of blockage were observed in biocide adapted sub-isolates compared to no biocide controls (Fig. 2).

Discussion

Using adaptive laboratory evolution, this study has demonstrated that mutations we have previously linked to CHD tolerance in *P. mirabilis* can be selected by exposure to both CHD and OCT and further extends our understanding of this process by providing new insight into mechanisms that underpin reduced susceptibility to these biocides. Of particular prominence in all biocide adapted populations generated were mutations predicted to inactivate the *smvR* repressor. Our previous work with the CHD tolerant *P. mirabilis* clinical isolate RS47 has already highlighted the importance of *smvR* inactivation to reduced CHD susceptibility in *P. mirabilis* and confirmed that mutations inactivating this repressor arise naturally in the clinical environment (Pelling et al. 2019). Inactivation of *smvR* leads to overexpression of the cognate *smvA* efflux pump, which is hypothesized to provide protection from CHD that penetrates the outer membrane and enters the periplasmic space (Pelling et al. 2019, Clarke et al. 2023). However, it should be noted that although we assume that elevated *smvA* gene expression correlates with an increase in the number of SmvA pumps embedded in the cytoplasmic membrane, additional posttranscriptional and posttranslational regulatory processes may modulate this, and increased mRNA production does not always lead to increased protein production.

The prevalence of *smvR* inactivation in our adapted populations is also congruent with studies in other species, which have shown CHD adapted *Klebsiella pneumoniae*, *Klebsiella oxytoca*, *Citrobacter freundii*, and *Salmonella enterica* Serovar Enteritidis acquire similar mutations in *smvR* (Wand et al. 2016, 2019). This includes mutations in both the *smvR* open reading frame (predicted to lead to a truncated product) as well as mutations in the promoter region (expected to

reduce gene expression) as observed in our *P. mirabilis* adaptation experiments. Similarly, adaptation of *Pseudomonas aeruginosa* to OCT has been reported to lead to acquisition of *smvR* mutations (Bock et al. 2021).

Moreover, our complementation studies with the OCT adapted RS50a$_{OCT3}$ sub-isolate, where *smvR* activity was restored and *smvA* expression suppressed, confirmed the importance of *smvA* mediated efflux in modulating both CHD and OCT susceptibility in *P. mirabilis*. The identification of a common mechanism modulating susceptibility to both OCT and CHD adds to accumulating evidence that *smvA* overexpression is a key mechanism modulating bacterial susceptibility to a range of cationic biocides, across multiple Gram-negative species (Slipski et al. 2018, Pelling et al. 2019, Wand et al. 2019, Bock et al. 2021). In contrast, the SmvAR system does not appear to contribute to changes antibiotic susceptibility in *P. mirabilis*, which is congruent with our previous work in *P. mirabilis*, and results from studies in a range of other species demonstrating changes in *smvAR* expression did not impact antibiotic susceptibility (Pelling et al. 2019, Wand et al. 2019, 2022, Guerin et al. 2020, Clarke et al. 2023). This suggests that *smvA* overexpression specifically modulates susceptibility to cationic biocides but does not promote cross-resistance to antibiotics.

In addition to *smvR*, mutations in the *rppA* response regulator (part of the two-component *rppAB* system in *P. mirabilis)*, and the *mipA* gene (encoding the MltA-interacting protein), were associated with *P. mirabilis* biocide adaptation in this study. Mutations in *rppA* were highly prevalent in adapted populations derived from the RS50a parental isolate but were not observed in adapted populations from any other WT lineages. Also of note in this regard is the conserved nature of *rppA* mutations observed in biocide adapted RS50a (which were all identical SNPs leading to D211N substitutions in RppA), and the ~64-fold increase in PMB MIC in RS50a biocide adapted sub-isolates linked with this mutation. Because susceptibility to PMB in *P. mirabilis* is known to be regulated by the *rppAB* system, and mutants defective in RppA activity display considerably greater susceptibility to PMB (Wang et al. 2008), there is strong evidence that the *rppA* SNPs selected for by biocide adaptation in RS50a restore or enhance the function of this regulator relative to the parental WT.

In turn, this indicates that a functional *rppAB* system is important for *P. mirabilis* adaptation to CHD and OCT. Although the *rppAB* system regulates a range of processes in *P. mirabilis*, perhaps of most relevance to CHD and OCT susceptibility is its role in regulating modification of lipid A with 4-amino-4-deoxy-L-arabinose (L-Ara4N) moieties, resulting in an increase in LPS net positive charge (Wang et al. 2008, Jiang et al. 2010, Olaitan et al. 2014). This in turn reduces binding of cationic peptides through electrostatic repulsion, and has been identified as the key mechanism underlying the innate resistance of *P. mirabilis* to antibiotics such as polymyxin B and colistin (Wang et al. 2008, Jiang et al. 2010). It has been suggested that the same electrostatic repulsion mechanisms may provide protection against other cationic antimicrobials, and inhibit penetration of CHD and OCT through the outer membrane (Wang et al. 2008). In keeping with this hypothesis are comparable observations in *K. pneumoniae*, where adaptation to increasing concentrations of CHD has been linked with mutations leading to upregulation of L-Ara4N addition to lipid A, and colistin resistance (Wand et al. 2016).

However, complementation studies with the RS50a$_{OCT3}$ sub-isolate, which encoded mutations in both *smvR* and *rppA*, did not support this hypothesis in *P. mirabilis*. Restoration of *smvA* activity in this sub-isolate (through complementation with a functional copy of *smvR*) fully restored susceptibility to both OCT and CHD despite the presence of the gain of function D211N RppA substitution. Overall, these experiments indicated that the gain of RppA activity in biocide adapted RS50a does not contribute directly to modulation of CHD or OCT susceptibility. Therefore, although a functional *rppAB* system appears to be associated with CHD and OCT adaptation in *P. mirabilis*, further work will be required to elucidate the exact role of this system in modulation of biocide susceptibility. This could include the possibility that a functional *rppAB* system is permissive for biocide adaptation, supporting or stabilizing the acquisition of mutations that directly modulate biocide susceptibility.

Mutations in *mipA* were associated with biocide adaptation in all isolates used in this study, but were only observed in CHD adapted populations, and were less prevalent than mutations in *smvR*. An analogous *mipA* mutation was also identified in the previously characterized CHD tolerant *P. mirabilis* RS47 (Pelling et al. 2019), and mutations in *mipA* have been reported in *K. pneumoniae* and *Enterobacter cloacae* following CHD exposure, as well as in biocide adapted *S. enterica* serovar Typhimurium (Curiao et al. 2016, Wand et al. 2016, 2019, Lescat et al. 2022). Furthermore, characterization of the biocide adapted sub-isolates RS50a$_{CHD8}$ and RS50a$_{OCT3}$ provided clear evidence that *mipA* mutations can contribute to reduced CHD susceptibility in *P. mirabilis*. Conversely, our data also indicates that MipA inactivation is not essential for *P. mirabilis* adaptation to CHD, since adapted sub-isolates lacking *mipA* mutations also exhibited the maximum CHD MICs observed. However, it should be noted in this regard that solubility of CHD limits the maximum concentration tested in MICs to 512 μg ml^{-1}, and it is conceivable that biocide adapted sub-isolates harbouring *mipA* mutations may exhibit greater CHD tolerance at concentrations above 512 μg ml^{-1}.

The mechanism through which *mipA* inactivation may contribute to reduced CHD susceptibility also remains unclear and will require further study to elucidate. The *mipA* gene encodes a putative structural MltA-interacting protein, which plays a role in peptidoglycan synthesis by aiding the formation of a multi-enzyme complex. This includes membrane-bound lytic transglycosylase (MltA) and murein (peptidoglycan) polymerase penicillin binding protein 1B (PBP1B) (Vollmer et al. 1999). The majority of *mipA* mutations observed in this study resulted in premature stop codons, which are expected to lead to the production of a truncated protein. This would be expected to impede formation of the MltA-PBP1B enzyme complex and therefore affect coordination of peptidoglycan synthesis (Vollmer et al. 1999).

If so, one possibility is that inactivation or truncation of MipA may confer protection to CHD though loss of particular cell envelope conformations generated by formation of the MltA-PBP1B enzyme complex. Because MltA is found in the outer membrane and PBP1B is linked to the cytoplasmic membrane, it has been proposed that MipA mediated

coupling of these enzymes leads to the formation of membrane adhesion sites, also termed Bayer junctions, which bring inner and outer membranes into close proximity (Vollmer et al. 1999). It is conceivable that the existence of such junctions may provide points at which CHD may more readily penetrate and interact with the cytoplasmic membrane, and the loss of these through MipA inactivation confers some protection. The predicted loss of the MltA-PBP1B complex in *mipA* mutants would also be expected to impact the coordination of peptidoglycan synthesis and lead to changes in peptidoglycan density, growth rate, and configuration that may also contribute to reduced CHD susceptibility. Alternatively, *mipA* encodes OmpV family conserved domains and is predicted to contain a large extracellular region spanning over half of the protein (Zhang et al. 2015, Han et al. 2020). In *P. mirabilis* biocide adapted *mipA* mutants, this extracellular domain is expected to be lost to different extents, raising the possibility that *mipA* may also play a more direct role in facilitating entry of CHD into the cell, with its inactivation reducing biocide entry.

In addition to the mechanisms relating to reduced biocide susceptibility in bacterial pathogens, there is also growing interest in the potential for biocide adaptation to modulate other traits, including virulence. In this regard, crystalline biofilm formation and blockage of catheters represents one of the key clinical problems resulting from *P. mirabilis* CAUTI (Stickler et al. 2014). However, our bladder model experiments showed no impact of mutations associated with this particular method of biocide adaptation on the ability to block catheters. Whilst we demonstrate that biocide adaptation can occur in response to exposure to escalating biocide concentrations, this is not necessarily reflective of a clinical environment. In a real-world scenario, isolates are likely to experience longer-term exposure to low level biocide concentrations or will experience sporadic exposure to high concentrations, followed by longer periods with no biocide exposure. Nevertheless, mutations in *smvR* and *mipA* are present in the highly CHD tolerance clinical isolate RS47, showing these emerge under real-world conditions and supporting the general utility of the directed evolution approach used here. Overall, our data have provided new insight into the adaptation of *P. mirabilis* to important antimicrobial agents and indicate that mechanisms underpinning the reduced susceptibility to CHD and OCT do not compromise the ability of this pathogen to encrust and block urethral catheters.

Supplementary data

Supplementary data is available at *JAMBIO Journal* online.

Conflict of interest: No conflict of interest declared.

Funding

This work was primarily supported by funding from the Medical Research Council and the UK Health Security Agency as an iCASE studentship to H.P. (MR/P015956/1) and funding from the Medical Research Council GW4 Biomed DTP as a studentship to V.B. (MR/N0137941/1). B.V.J. is also supported by funding from the Dunhill Medical Trust (RPGF1906\171).

Author contributions

Harriet Pelling (Conceptualization, Data curation, Formal analysis, Investigation, Methodology, Validation, Visualization, Writing – original draft), Vicky Bennett (Data curation, Formal analysis, Investigation, Methodology, Validation, Visualization, Writing – original draft, Writing – review & editing), Lucy J. Bock (Conceptualization, Supervision), Matthew E. Wand (Conceptualization, Supervision), Emma L. Denham (Supervision), Wendy M. MacFarlane (Supervision), J. Mark Sutton (Conceptualization, Supervision), and Brian V. Jones (Conceptualization, Data curation, Formal analysis, Funding acquisition, Methodology, Project administration, Resources, Supervision, Visualization, Writing – original draft, Writing – review & editing)

Data availability

Raw reads for parental isolates are available under BioProject accession number PRJNA554808. The complete annotated genome assembly for *P. mirabilis* HI4320 is available under BioProject accession number PRJNA608758.

References

Afgan E, Baker D, Batut B *et al*. The Galaxy platform for accessible, reproducible and collaborative biomedical analyses: 2018 update, *Nucleic Acids Res*, 2018; **46**:W537–44. https://doi.org/10.1093/nar/gky379

Atiyeh BS, Dibo SA, Hayek SN. Wound cleansing, topical antiseptics and wound healing. *Int Wound J* 2009;**6**:420–30. https://doi.org/10.1111/j.1742-481X.2009.00639.x

Blum M, Chang H-Y, Chuguransky S *et al*. The InterPro protein families and domains database: 20 years on *Nucleic Acids Res* 2021;**49**:D344–54. https://doi.org/10.1093/nar/gkaa977

Bock LJ, Ferguson PM, Clarke M *et al*., *Pseudomonas aeruginosa* adapts to octenidine via a combination of efflux and membrane remodelling. *Commun Biol* 2021;**4**:1058. https://doi.org/10.1038/s42003-021-02566-4

Bock LJ, Hind CK, Sutton JM *et al*. Growth media and assay plate material can impact on the effectiveness of cationic biocides and antibiotics against different bacterial species. *Lett Appl Microbiol* 2018;**66**:368–77. https://doi.org/10.1111/lam.12863

Bock LJ, Wand ME, Sutton JM. Varying activity of chlorhexidine-based disinfectants against *Klebsiella pneumoniae* clinical isolates and adapted strains. *J Hosp Infect* 2016;**93**:42–48. https://doi.org/10.1016/j.jhin.2015.12.019

Chen S, Zhou Y, Chen Y *et al*. FastP: an ultra-fast all-in-one-FASTQ preprocessor. *Bioinformatics* 2018;**34**:i884–90 https://doi.org/10.1093/bioinformatics/bty560

Clarke OE, Pelling H, Bennett V *et al*. Lipopolysaccharide structure modulates cationic biocide susceptibility and crystalline biofilm formation in *Proteus mirabilis*. *Front Microbiol* 2023;**14**:1150625 https://doi.org/10.3389/fmicb.2023.1150625

Coaguila-Llerena H, Rodrigues EM, Santos CS *et al*. Effects of octenidine applied alone or mixed with sodium hypochlorite on eukaryotic cells. *Int Endodontic J* 2020;**53**:1264–74. https://doi.org/10.1111/iej.13347

Coia JE, Wilson JA, Bak A *et al*. Joint Healthcare Infection Society (HIS) and Infection Prevention Society (IPS) guidelines for the prevention and control of meticillin-resistant Staphylococcus aureus (MRSA) in healthcare facilities. *J Hosp Infect* 2021;**118**:S1–S39 https://doi.org/10.1016/j.jhin.2021.09.022

Curiao T, Marchi E, Grandgirard D *et al*. Multiple adaptive routes of *Salmonella enterica* Typhimurium to biocide and antibiotic exposure. *BMC Genomics [Electronic Resource]* 2016;**17**:491. https://doi.org/10.1186/s12864-016-2778-z

Dance DA, Pearson AD, Seal DV *et al*. A hospital outbreak caused by a chlorhexidine and antibiotic-resistant *Proteus mirabilis*. *J Hosp Infect* 1987;**10**:10–16. https://doi.org/10.1016/0195-6701(87)90027-2

Danecek P, Bonfield J, Liddle J *et al*. Twelve years of SAMtools and BCFtools *GigaScience* 2021;**10**:giab008. https://doi.org/10.1093/gigascience/giab008

Deatherage DE, Barrick JE. Identification of mutations in laboratory-evolved microbes from next-generation sequencing data using breseq. *Methods Mol Biol*. 2014;**1151**:165–88. https://doi.org/10.1007/978-1-4939-0554-6_12

Garrison E, Marth G. Haplotype-based variant detection from short-read sequencing. 2012. arXiv preprint:1207.3907[q-bio.GN].

Gilbert P, Moore LE. Cationic antiseptics: diversity of action under a common epithet. *J Appl Microbiol* 2005;**99**:703–15. https://doi.org/10.1111/j.1365-2672.2005.02664.x

Gillespie WA, Lennon GG, Linton KB *et al*. Prevention of urinary infection by means of closed drainage into a sterile plastic bag. *Br Med J* 1967;**3**:90–92. https://doi.org/10.1136/bmj.3.5557.90

Guerin F, Gravey F, Plésiat P *et al*. The Transcriptional repressor SmvR is important for decreased chlorhexidine susceptibility in *Enterobacter clocase* complex. *Antimicrob Agents Chemother* 2020;**64**:e01845–19. https://doi.org/10.1128/AAC.01845-19

Han MJ. Novel bacterial surface display system based on the *Escherichia coli* protein MipA. *J Microbiol Biotechnol* 2020;**30**:1097–103. https://doi.org/10.4014/jmb.2001.01053

Harbarth S, Tuan Soh S, Horner C *et al*. Is reduced susceptibility to disinfectants and antiseptics a risk in healthcare settings? A point/counterpoint review. *J Hosp Infect* 2014;**87**:194–202. https://doi.org/10.1016/j.jhin.2014.04.012

Hardy K, Sunnucks K, Gil H *et al*. Increased usage of antiseptics is associated with reduced susceptibility in clinical isolates of *Staphylococcus aureus*. *mBio* 2018;**9**:e00894–18. https://doi.org/10.1128/mBio.00894-18

Jacobsen SM, Stickler DJ, Mobley HL *et al*. Complicated catheter-associated urinary tract infections due to *Escherichia coli* and *Proteus mirabilis*. *Clin Microbiol Rev* 2008;**21**:26–59. https://doi.org/10.1128/CMR.00019-07

Jiang SS, Liu MC, Teng LJ *et al*. *Proteus mirabilis* pmrI, an RppA-regulated gene necessary for polymyxin B resistance, biofilm formation, and urothelial cell invasion. *Antimicrob Agents Chemother* 2010;**54**:1564–71. https://doi.org/10.1128/AAC.01219-09

Kampf G. Acquired resistance to chlorhexidine—is it time to establish an 'antiseptic stewardship' initiative? *J Hosp Infect* 2016;**94**:213–27. https://doi.org/10.1016/j.jhin.2016.08.018

Lai NM, Lai NA, O'Riordan E *et al*. Skin antisepsis for reducing central venous catheter-related infections. *Cochrane Database Syst Rev* 2016;**7**:CD010140.

Lambert PA, Mechanisms of action of microbicides. In: Fraise A.P., Maillard J.-Y., Sattar S.A. eds, *Russell, Hugo and Ayliffe's Principles and Practice of Disinfection, Preservation and Sterilization*. 5th edn. Chichester (UK): Wiley-Blackwell, 2012;95–107.

Lescat M, Magnan M, Kenmoe S *et al*. Co-lateral effect of octenidine, chlorhexidine and colistin selective pressures on four enterobacterial species: a comparative genomic analysis. *Antibiotics* 2022;**11**:50.

Lim KS, Kam PC. Chlorhexidine—pharmacology and clinical applications. *Anaesth Intensive Care* 2008;**36**:502–12. https://doi.org/10.1177/0310057X0803600404

Maillard J-Y. Antimicrobial biocides in the healthcare environment: efficacy, usage, policies, and perceived problems. *Ther Clinl Risk Manag* 2005;**1**:307–20.

McDonnell G, Russell AD. Antiseptics and disinfectants: activity, action, and resistance. *Clin Microbiol Rev* 1999;**12**:147–79. https://doi.org/10.1128/CMR.12.1.147

Morris NS, Stickler DJ. Encrustation of indwelling urethral catheters by *Proteus mirabilis* biofilms growing in human urine. *J Hosp Infect* 1998;**39**:227–34. https://doi.org/10.1016/S0195-6701(98)90262-6

Murray CJL, Ikuta KS, Sharara F *et al*. Global burden of bacterial antimicrobial resistance in 2019: a systematic analysis. *Lancet North Am Ed* 2022;**399**:629–55. https://doi.org/10.1016/S0140-6736(21)02724-0

NICE. Healthcare-associated infections: prevention and control in primary and community care. 2017. CG139. https://www.nice.org.uk/guidance/cg139 (22 September 2021, date last accessed).

NICE. Surgical site infections: prevention and treatment. 2020. NG125. https://www.nice.org.uk/guidance/ng125 (22 September 2021, date last accessed).

O'Flynn JD, Stickler DJ. Disinfectants and gram-negative bacteria. *Lancet North Am Ed* 1972;**299**:489–90. https://doi.org/10.1016/S0140-6736(72)90142-0

Olaitan AO, Morand S, Rolain JM. Mechanisms of polymyxin resistance: acquired and intrinsic resistance in bacteria. *Front Microbiol* 2014;**5**:643. https://doi.org/10.3389/fmicb.2014.00643

Pelling H, Bock LJ, Nzakizwanayo J *et al*. De-repression of the smvA efflux system arises in clinical isolates of *Proteus mirabilis* and reduces susceptibility to chlorhexidine and other biocides. *Antimicrob Agents Chemother* 2019;**63**:e01535–19 https://doi.org/10.1128/AAC.01535-19

Prjibelski A, Antipov D, Meleshko D *et al*. Using SPAdes de novo assembler. *Curr Protoc Bioinformatics* 2020;**70**:e102 https://doi.org/10.1002/cpbi.102

Rawson TM, Moore LSP, Zhu N *et al*. Bacterial and fungal coinfection in individuals with coronavirus: a rapid review to support COVID-19 antimicrobial prescribing. *Clin Infect Dis* 2020;**71**:2459–68.

Russell AD. Chlorhexidine: antibacterial action and bacterial resistance. *Infection* 1986;**14**:212–5. https://doi.org/10.1007/BF01644264

Schmidt J, Zyba V, Jung K *et al*. Cytotoxic effects of octenidine mouth rinse on human fibroblasts and epithelial cells—an in vitro study. *Drug Chem Toxicol* 2016;**39**:322–30. https://doi.org/10.3109/01480545.2015.1121274

Schmidt J, Zyba V, Jung K *et al*. Effects of octenidine mouth rinse on apoptosis and necrosis of human fibroblasts and epithelial cells—an in vitro study. *Drug Chem Toxicol* 2018;**41**:182–7. https://doi.org/10.1080/01480545.2017.1337124

Schülke & Mayr UK Ltd. Products for Infection Prevention. 2021. https://www.schuelke.com/gb-en/infection-prevention/products/products_IP_landing-page.php?navid=783761498278 (21 September 2021, date last accessed).

Slipski CJ, Zhanel GG, Bay DC. Biocide selective TolC-independent efflux pumps in Enterobacteriaceae. *J Membrane Biol* 2018;**251**:15–33. https://doi.org/10.1007/s00232-017-9992-8

Southampton Infection Control Team. Evaluation of aseptic techniques and chlorhexidine on the rate of catheter-associated urinary-tract infection. *Lancet North Am Ed* 1982;**319**:89–91. https://doi.org/10.1016/S0140-6736(82)90224-0

Stickler D, Ganderton L, King J *et al*. *Proteus mirabilis* biofilms and the encrustation of urethral catheters. *Urol Res* 1993;**21**:407–11. https://doi.org/10.1007/BF00300077

Stickler DJ, Evans A, Morris N *et al*. Strategies for the control of catheter encrustation. *Int J Antimicrob Agents* 2002;**19**:499–506. https://doi.org/10.1016/S0924-8579(02)00091-2

Stickler DJ, Feneley RC. The encrustation and blockage of long-term indwelling bladder catheters: a way forward in prevention and control. *Spinal Cord* 2010;**48**:784–90. https://doi.org/10.1038/sc.2010.32

Stickler DJ, Morris NS, Winters C. [35] Simple physical model to study formation and physiology of biofilms on urethral catheters. *Methods Enzymol* 1999;**310**:494–501. https://doi.org/10.1016/S0076-6879(99)10037-5

Stickler DJ, Thomas B. Antiseptic and antibiotic resistance in Gram-negative bacteria causing urinary tract infection. *J Clin Pathol* 1980;**33**:288–96. https://doi.org/10.1136/jcp.33.3.288

Stickler DJ. Chlorhexidine resistance in *Proteus mirabilis*. *J Clin Pathol* 1974;**27**:284–7. https://doi.org/10.1136/jcp.27.4.284

Stickler DJ. Clinical complications of urinary catheters caused by crystalline biofilms: somethings needs to be done. *J Intern Med* 2014;**276**:120–9 https://doi.org/10.1111/joim.12220

Vollmer W, von Rechenberg M, Höltje J-V. Demonstration of molecular interactions between the murein polymerase PBP1B, the lytic transglycosylase MltA, and the scaffolding protein MipA of *Escherichia coli*. *J Biol Chem* 1999;**274**:6726–34. https://doi.org/10.1074/jbc.274.10.6726

Walker EM, Lowes JA. An investigation into in vitro methods for the detection of chlorhexidine resistance. *J Hosp Infect* 1985;**6**:389–97. https://doi.org/10.1016/0195-6701(85)90055-6

Wand M, Darbym E, Blair J *et al*. Contribution of the efflux pump AcrAB-TolC to the tolerance of chlorhexidine and other biocides in Klebsiella spp.. *J Med Microbiol* 2022;71. https://doi.org/10.1099/jmm.0.001496

Wand ME, Bock LJ, Bonney LC *et al*. Mechanisms of increased resistance to chlorhexidine and cross-resistance to colistin following exposure of *Klebsiella pneumoniae* clinical isolates to chlorhexidine. *Antimicrob Agents Chemother* 2016;**61**:e01162–16.

Wand ME, Jamshidi S, Bock LJ *et al*. SmvA is an important efflux pump for cationic biocides in *Klebsiella pneumoniae* and other Enterobacteriaceae. *Sci Rep* 2019;**9**:1344. https://doi.org/10.1038/s41598-018-37730-0

Wang WB, Chen IC, Jiang SS *et al*. Role of RppA in the regulation of polymyxin b susceptibility, swarming, and virulence factor expression in *Proteus mirabilis*. *Infect Immun* 2008;**76**:2051–62. https://doi.org/10.1128/IAI.01557-07

WHO. Global trends—bacteria, resistance in bacteria. 2017. http://www.euro.who.int/en/health-topics/disease-prevention/antimicrobial-resistance/about-amr/global-trends-bacteria (11 August 2017, date last accessed).

WHO. WHO model list of essential medicines. 2021. https://www.who.int/publications/i/item/WHO-MHP-HPS-EML-2021.02 (20 November 2021, date last accessed).

Zhang D-f, Li H, Lin X-m *et al*. Outer membrane proteomics of kanamycin-resistant *Escherichia coli* identified MipA as a novel antibiotic resistance-related protein. *FEMS Microbiol Lett* 2015;**362**:fnv074. https://doi.org/10.1093/femsle/fnv074

Zheng G, Filippelli GM, Salamova A. Increased indoor exposure to commonly used disinfectants during the COVID-19 pandemic. *Environ Sci Technol Lett* 2020;**7**:760–5

Received 10 May 2024; **revised** 20 June 2024; **accepted** 10 July 2024